NUCL SCI TECH (2018) 29:102
https://doi.org/10.1007/s41365-018-0430-0

Investigation of high-temperature-resistant rhenium–boron neutron shields by experimental studies and Monte Carlo simulations

Turgay Korkut[1] · Hatun Korkut[1] · Bünyamin Aygün[2] · Özkan Bayram[3] · Abdulhalik Karabulut[2,4]

Received: 31 May 2017 / Revised: 27 October 2017 / Accepted: 15 November 2017 / Published online: 30 May 2018

Abstract In this study, novel rhenium–boron neutron-shielding high-temperature-resistant materials were designed. The considered samples, Re60–B40, Re58–B42, Re50–B50, and Re40–B60, with different concentrations of rhenium and boron were investigated to elucidate their neutron-shielding performances, and compare them with well-known neutron-shielding materials such as the 316LN quality nuclear steel. In addition to the experimental studies, Monte Carlo simulations were performed using the FLUKA and GEANT4 codes, where 4.5-MeV neutrons emitted by a ^{241}Am–Be source were employed. Experimental equivalent dose rates, simulated track lengths, energy balances, and neutron mass absorption cross sections were discussed in detail.

Keywords Rhenium · Boron · Nuclear protection · Neutrons · Monte Carlo simulation

This work was supported by the Scientific and Technological Research Council of Turkey (TUBITAK) (No: 111T764).

✉ Turgay Korkut
turgaykorkut@hotmail.com

1 Department of Nuclear Energy Engineering, Faculty of Engineering, Sinop University, 57000 Sinop, Turkey

2 Department of Physics, Faculty of Science, Atatürk University, 25040 Erzurum, Turkey

3 Department of Materials Sciences and Nanotechnology Engineering, Faculty of Engineering, Bayburt University, 69000 Bayburt, Turkey

4 Ağrı İbrahim Çeçen University, 04000 Ağrı, Turkey

1 Introduction

In the design of nuclear power plants, piping systems with high radiation, pressure, and temperature resistances are of key importance. Martin and Reid studied molybdenum-rhenium (44.5%) alloys as reactor heat pipe materials [1]. In addition, rhenium-containing alloys have been used in nuclear fusion applications and atom probe tomography (APT) system components [2]. Bulk ^{186}Re has been irradiated with accelerated protons at the Los Alamos National Laboratory for clinical radiotherapy applications; the results were studied by Mastren et al. [3]. Another research revealed that the mechanical strength of steel was not affected by the presence of rhenium, while its radiation shielding properties improved with the increase in the rhenium concentration in stainless steel (9Cr–2W–0.25V–0.07Ta–0.1C). [4]. High-temperature neutron irradiation of molybdenum–rhenium welds was studied by Krajnikov et al. They revealed a significant increase in microrigidity of the molybdenum-rhenium alloys at both low and high temperatures, attributed to the neutron irradiation [5]. Corr et al. [6] revealed that the Re-ion irradiation and He-plasma application created a large increase in hardness of the irradiated tungsten target. In addition, rhenium-based and boron-containing materials were used as nuclear protection materials, in particular, against neutrons [7, 8]. Boron-containing and boron-based nuclear shields have been extensively investigated, which revealed their excellent properties.

High-technology materials with excellent heat-resistant and neutron-shielding capacities are required for applications in nuclear technologies. They are of key importance for fission- and fusion-based power plants. Newly fabricated samples with a high level of rhenium exhibit a high-temperature resistance and almost perfect shielding capacity. In addition, it has been reported that rhenium is a perfect nuclear shield [9]. Therefore, rhenium is used as a basic material of newly fabricated neutron-shielding samples encoded as Re60–B40, Re58–B42, Re50–B50, and Re50–B50 according to their elemental composition. Rhenium (Re) is the most commonly used silvery-white refractory metal with an atomic number (*Z*) of 75. It is a transition metal with excellent temperature resistance and hardness. It is used in nuclear technologies for various applications, from space equipment to nuclear reactor shields. Rhenium–molybdenum alloys are frequently used in various industrial field including nuclear medicine. Rhenium-containing and rhenium-based alloys are promising owing to their perfect shielding properties and high-temperature resistance. For example, an iridium-coated rhenium (Ir/Re) burning chamber achieves hours of operation up to temperatures of 2200 °C. It offers the required thermal tolerance for high-capacity long-life radiation-cooled rockets [10]. Boron (B) is a low-*Z* chemical element; its compounds and minerals are widely used in nuclear reactors for neutron moderation purposes and boron neutron capture therapy applications.

In this study, novel high-temperature-resistant neutron-shielding materials were designed using the FLUKA [11, 12, 23] and GEANT4 [13, 14, 22] software packages, which are Monte Carlo simulation codes; they can model materials with different rhenium–boron ratios. Experimental equivalent dose rates were measured. Owing to its perfect shielding parameters, the 316LN quality nuclear steel was chosen as a reference material for comparison.

2 Materials and methods

2.1 Geant4

GEANT4 is a widely used Monte Carlo package for the simulation of transfer of particles through matter. It is employed in high-energy-particle plasma physics, nuclear applications, accelerator modelling, medical physics, cosmic ray physics, etc. In this code, neutrons are simulated using four different high-precision (HP) data-driven hadronic physics models (G4NeutronHPElastic, G4NeutronHPInelastic, G4NeutronHPCapture, and G4NeutronHPFission). In the GEANT4 input files, neutrons can be defined to have an energy in the range of 0.025 eV (thermal region) to 20 MeV (fast region). In this study, the Geant4.10.02.p01 version of the code was used to estimate the neutron–sample interactions.

2.2 Fluka

FLUKA is one of the Monte Carlo codes that very accurately model electromagnetic, cosmic, and nuclear interactions for all materials. It is widely used in high-energy particle physics, shielding, detector design, modelling cosmic ray interactions, medical dosimetry, radiobiology, radiation protection, etc. We used the FLUKA Monte Carlo code to determine absorbed doses, macroscopic cross sections, neutron fluencies, and produced radioisotopes by samples after neutron irradiation. In this study, the FLUKA.2011.2b.6 version was used.

The GEANT4 and FLUKA Monte Carlo codes were previously used in our studies on gamma and neutron shielding [15–20]. GEANT4 and FLUKA differ from each other in terms of neutron transport. FLUKA uses its own cross-sectional libraries, while GEANT4 uses the hadron physics (HP) ENDF (evaluated nuclear data file) library. Cross-sectional models and neutron energy limits libraries are used in the two codes.

2.3 Simulation setup

The samples were modelled using the FLUKA and GEANT4 Monte Carlo simulation codes. GEANT4 and FLUKA simulations were performed to estimate neutron absorption cross sections ($\sum_{R}/\rho\,(\mathrm{cm}^2/\mathrm{g}) - \sum_{R}$ effective removal cross section, ρ density of sample), total track lengths, and energy balances. The dimensions of the sample were set to 10 × 10 × 10 mm^3. Boron was added in the rhenium sample at different weight percentages; owing to its high neutron total macroscopic cross section 10-μCi ^{241}Am–Be neutrons were used in the simulations. A total of 260 neutron cross-sectional libraries are used in FLUKA; the G4NDL3.14 neutron cross-sectional library is selected for the GEANT4 simulations. An image of the experimental setup and illustration of the employed geometry in the theoretical simulations are shown in Fig. 1.

2.4 Sample preparation

In this study, neutron-shielding capacities of rhenium–boron structures were investigated. We prepared four samples with different percentages of boron in rhenium. All of them had a mass of 2.5 g and diameter of 2 cm. Rhenium and boron powders were milled for 3 h. After pelleting using the SPECAC hydraulic press equipment at 600 MPa, the disc samples were annealed at 1200 °C for 6 h. The sample names, their densities, and B–Re percentages are listed in Table 1. The produced samples are shown in Fig. 2.

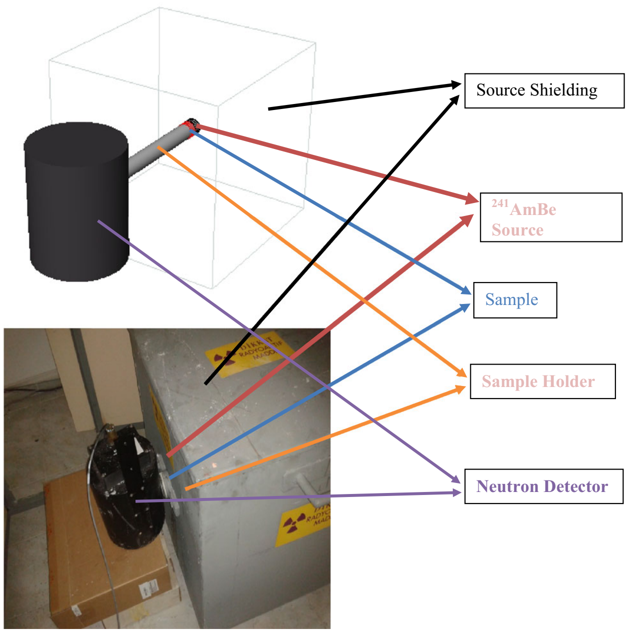

Fig. 1 (Color online) Simulation geometry and experimental setup

Table 1 Names, weight compositions, and densities of the samples

Sample name	Rhenium (%)	Boron (%)	ρ (g/cm^3)
Re60–B40	60	40	13.55
Re58–B42	58	42	13.17
Re50–B50	50	50	11.68
Re40–B60	40	60	9.81

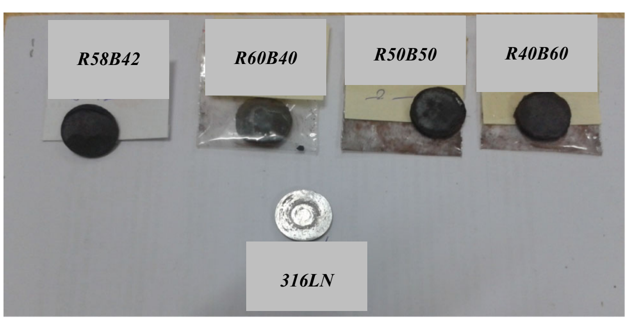

Fig. 2 (Color online) Produced samples

2.5 Experimental methods

In the neutron equivalent dose rate experiments, a ^{241}Am/Be neutron source (10 mCi) and Canberra neutron detector were used. The ^{241}Am/Be source emits 2–11 MeV energetic neutrons. The conventional ^{241}Am/Be neutron source is a mixture of americium dioxide and beryllium metal powders. The NP-100B detector system [boron trifluoride-(BF_3)-filled neutron detector] can detect over a wide energy range, from slow to fast neutrons. Equivalent dose rate results were obtained using the radiological assessment display and control system (RADACS) software on the system PC. The experimental setup comprises a neutron source, neutron detector, and sample, as shown in Fig. 1. The detector is placed 30 cm in front of the source.

The mass absorption cross section can be calculated from $\sum_R/\rho$, where $\sum_R$ is the effective removal cross section

$$\sum_R = \sum_i \rho_i \left(\sum_R/\rho\right)_i,$$

and ρ is the density of the sample [21].

3 Results and discussion

3.1 Monte Carlo simulation results

Table 2 shows the results for the two shielding parameters, total particle track length and energy balance after the interactions. GEANT4 was used to estimate the total track length (l_t) after the particle–sample interactions; it is calculated (see GEANT4 manual) as the sum of the step lengths in the cell:

$$l_t = s_i/wf_i,$$

where s_i is the collision score, w is the neutron weight, and f_i is the value of the response function. The results show that the total track length decreases with the decrease in the rhenium percentage in the sample, which implies that the neutron flux decreases. The lower neutron flux implies that the sample is a good neutron-shielding material. Therefore, among the considered samples, Re40–B60 is the best neutron-shielding material.

Next, energy balance is the sum of deposited energy and energy leakage; it corresponds to the Q value of a nuclear reaction

$$x + X \rightarrow y + Y + Q\,(\text{MeV}) + \cdots$$

The energy balance (Q) reveals the absorbed dose in the sample. Therefore, high-performance shielding materials exhibit a high energy balance owing to the high absorbed dose rate. Table 2 shows the energy balance results for all samples. The energy balance increases with the decrease in the rhenium percentage, which further confirms that Re40–B60 is the best neutron-shielding sample. Table 3 shows the neutron mass absorption cross sections, which support the above results. The neutron-shielding capacity of the Re40–B60 sample, which has a high neutron mass absorption cross section (Σ/ρ), is higher than those of the other samples.

Table 2 Shielding parameters obtained using the Monte Carlo simulations

Sample	Total track length (cm) (GEANT4)	Error	Energy balance (MeV) (GEANT4)	Error
Re60–B40	1.127	± 0.0451	3.705	± 0.1482
Re58–B42	1.124	± 0.0449	3.710	± 0.1484
Re50–B50	1.108	± 0.0443	3.737	± 0.1495
Re40–B60	1.089	± 0.0435	3.784	± 0.1514

Table 3 4.5-MeV neutron mass absorption cross-sections of the samples

Sample	Σ/ρ (cm^2/g) (GEANT4)	Error	Σ/ρ (cm^2/g) (FLUKA)	Error	Difference between codes' results (%)
Re60–B40	0.052	± 0.0022	0.050	± 0.0017	2.71
Re58–B42	0.053	± 0.0021	0.051	± 0.0017	2.60
Re50–B50	0.059	± 0.0025	0.056	± 0.0019	4.93
Re40–B60	0.066	± 0.0027	0.064	± 0.0021	3.84

3.2 Equivalent dose rate results

According to the simulation results, four samples were fabricated, and equivalent dose rate measurements and Monte Carlo calculations were performed. The experimental equivalent dose rate and simulation results (absorbed by the detector) (in μSv/h) are shown in Fig. 3. In addition, the experimental equivalent dose rate results with statistical evaluation are shown in Table 4. The figure shows that the equivalent dose rate is the lowest for Re40–B60. A larger absorbed dose by the detector implies a lower absorbed dose by the sample. A low equivalent dose rate absorbed by the detector implies a high neutron-shielding capability of the sample. Therefore, Re40–B60 exhibits the largest neutron-shielding capability. It is worth noting that Re60–B40, Re58–B42, Re50–B50, and Re40–B60 exhibit better neutron-shielding capacities than that of the 316LN steel.

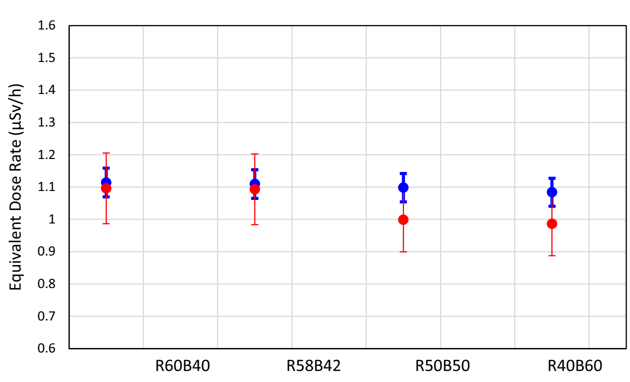

Fig. 3 (Color online) Neutron equivalent dose rate measurements, compared with FLUKA results

4 Conclusion

Monte Carlo simulations (FLUKA and GEANT4 codes) were performed to reveal neutron-shielding parameters of four samples. The neutron equivalent dose rates of these samples and 316LN quality nuclear steel were obtained by experiments and simulations. The high density and good neutron absorption capacity of the 316LN quality nuclear steel, used in the nuclear industry, make it a good reference material. The four samples (Re60–B40, Re58–B42, Re50–B50, and Re40–B60) had higher densities and neutron-shielding parameters, compared with those of the steel, as shown in Tables 3 and 4 and Fig. 3. Therefore, the four samples had excellent neutron-shielding performances. The simulation results of the neutron-shielding parameters, total track length and energy balance, confirmed the experimental results. The best sample properties were obtained with the lowest track length, highest energy balance, highest mass absorption cross section, and lowest experimental equivalent dose rate (absorbed by the detector). Accordingly, the Re40–B60 sample had the highest neutron-shielding capability. These findings could be useful in nuclear engineering, radiation shielding, and nuclear safety applications.

The neutron absorption capacity increased with the boron percentage in the composite. Boron has a higher neutron-shielding capacity than rhenium. Rhenium was added to the composite, owing to its high atomic number; rhenium addition increased the scattering cross section for fast neutrons. Therefore, the proposed composite material has improved neutron-shielding properties and larger neutron scattering cross section [22].

Table 4 Experimental equivalent dose rates

Sample	Equivalent dose rate (μSv/h)	Error	Standard deviation
Re60–B40	1.096	± 0.1096	0.7124
Re58–B42	1.093	± 0.1093	0.3226
Re50–B50	0.999	± 0.0999	0.6136
Re40–B60	0.986	± 0.0986	0.2277
316LN	1.175	± 0.1175	0.4365

Acknowledgements We wish to thank Prof. Gökhan Budak, who died on January 26, 2013, for his contributions to our studies and scientific world.

References

1. J.J. Martin, R.S. Reid, Life test approach for refractory metal/-sodium heat pipes. AIP Conf. Proc. **813**, 108–116 (2006). https://doi.org/10.1063/1.2169186
2. A. Xu, E.J. Armstrong David et al., Ion irradiation induced clustering in W–Re–Ta, W–Re and W–Ta alloys: an atom probe tomography and nano indentation study. Acta Mater. **124**, 71–78 (2017). https://doi.org/10.1016/j.actamat.2016.10.050
3. T. Mastrena, V. Radchenko et al., Bulk production and evaluation of high specific activity 186gRe for cancer therapy using enriched 186WO3 targets in a proton beam. Nucl. Med. Biol. **49**, 24–29 (2017). https://doi.org/10.1016/S0022-3115(99)00269-X
4. R.L. Klueh, D.J. Alexander et al., Effect of rhenium and osmium on mechanical properties of a 9Cr–2W–0.25V–0.07Ta–0.1C steel. J. Nucl. Mater. **279**(1), 91–99 (2000). https://doi.org/10.1016/S0022-3115(99)00269-X
5. A.V. Krajnikova, F. Moritob et al., Embrittlement of molybdenum–rhenium welds under low and high temperature neutron irradiation. J. Nucl. Mater. **444**(1–3), 404–415 (2014). https://doi.org/10.1016/j.jnucmat.2013.10.027
6. C.S. Corr, S.O. Ryan et al., Mechanical properties of tungsten following rhenium ion and helium plasma exposure. Nucl. Mater. Energy (2017). https://doi.org/10.1016/j.nme.2017.04.012 (**in press**)
7. H. Yiping, L. Lu et al., The design study of a new nuclear protection material. Nucl. Eng. Des. **248**, 22–27 (2012). https://doi.org/10.1016/j.nucengdes.2012.03.016
8. T. Korkut, A. Karabulut et al., Investigation of neutron shielding properties depending on number of boron atoms for colemanite, ulexite and tincal ores by experiments and FLUKA Monte Carlo simulations. Appl. Radiat. Isotopes **70**(1), 341–345 (2012). https://doi.org/10.1016/j.apradiso.2011.09.006
9. R.A. Karam, T.F. Parkinson et al., Final Technical Reports on the Nuclear Properties of Rhenium (1963). Department of Nuclear Engineering University of Florida Gainesville, Florida
10. S.X. Bai, L. Zhu et al., High-temperature diffusion in couple of chemical vapor deposited rhenium and electrodeposited iridium. Int. J. Refract. Met. H **41**(563–570), 2005 (2013). https://doi.org/10.1016/j.ijrmhm.2013.07.008
11. A. Ferrari, P.R. Sala et al., FLUKA: a multi-particle transport code. CERN-2005-10, INFN/TC_05/11, SLAC-R-773
12. G. Battistoni, S. Muraro et al., In: Proceedings of the Hadronic Shower Simulation Workshop 2006, Fermilab (6–8 September 2006)
13. S. Agostinelli, J. Allison et al., Geant4-a simulation toolkit. Nucl. Instrum. Methods A **506**, 250–303 (2003). https://doi.org/10.1016/S0168-9002(03)01368-8
14. J. Allison, K. Amako et al., Geant4 developments and applications. IEEE Trans. Nucl. Sci. **53**, 270–278 (2006). https://doi.org/10.1109/TNS.2006.869826
15. K.S. Mann, T. Korkut, Gamma-ray buildup factors study for deep penetration in some silicates. Ann. Nucl. Energy **51**, 81–93 (2013). https://doi.org/10.1016/j.anucene.2012.08.024
16. O. Gencel, A. Bozkurt et al., Determination and calculation of gamma and neutron shielding characteristics of concretes containing different hematite proportions. Ann. Nucl. Energy **38**(12), 2719–2723 (2011). https://doi.org/10.1016/j.anucene.2011.08.010
17. T. Korkut, H. Korkut, FLUKA simulations of DPA in 6H–SiC reactor blanket material induced by different radiation fields frequently mentioned in literature. J. Fusion Energy **32**(1), 66–70 (2013). https://doi.org/10.1007/s10894-012-9525-5
18. T. Korkut, H. Korkut et al., A new radiation shielding material: amethyst ore. Ann. Nucl. Energy **38**(1), 56–59 (2011). https://doi.org/10.1016/j.anucene.2010.08.017
19. T. Korkut, O. Gencel et al., X-ray, gamma, and neutron radiation tests on epoxy-ferrochromium slag composites by experiments and monte carlo simulations. Int J Polymer Anal Charact **18**, 224–231 (2013). https://doi.org/10.1080/1023666X.2013.755658
20. M.F. Kaplan, *Concrete Radiation Shielding: Nuclear Physics, Concrete Properties, Design and Construction* (Longman Scientific & Technical, New York, 1989)
21. A.B. Smith, Fast-neutron scattering from elemental rhenium. J. Phys. G Nucl. Part. Phys. **30**(4), 407 (2004). https://doi.org/10.1088/0954-3899/30/4/003
22. http://geant4.cern.ch/
23. http://www.fluka.org/fluka.php